International Journal of Solids and Structures 49 (2012) 919–928

Contents lists available at SciVerse ScienceDirect

International Journal of Solids and Structures

journal homepage: www.elsevier.com/locate/ijsolstr

Micromechanical analysis of damage in saturated quasi brittle materials

Ni Xie [a,b], Qi-Zhi Zhu [c], Jian-Fu Shao [b,*], Li-Hua Xu [a]

[a] School of Civil Engineering, Wuhan University, Wuhan, China
[b] Laboratory of Mechanics of Lille, UMR 8107 CNRS, University of Lille I, Cite Scientifique, 59655 Villeneuve d'Ascq, France
[c] Laboratoire Modélisation et Simulation Multi Echelle, MSME UMR 8208 CNRS, Université Paris-Est, 77454 Marne la Vallée, France

ARTICLE INFO

Article history:
Received 22 March 2011
Received in revised form 7 December 2011
Available online 24 December 2011

Keywords:
Damage
Micromechanics
Homogenization
Microcracks
Frictional sliding
Porous materials

ABSTRACT

In this paper, we propose a micromechanical analysis of damage and related inelastic deformation in saturated porous quasi brittle materials. The materials are weakened by randomly distributed microcracks and saturated by interstitial fluid with drained and undrained conditions. The emphasis is put on the closed cracks under compression-dominated stresses. The material damage is related to the frictional sliding on crack surface and described by a local scalar variable. The effective properties of the materials are determined using a linear homogenization approach, based on the extension of Eshelby's inclusion solution to penny shaped cracks. The inelastic behavior induced by microcracks is described in the framework of the irreversible thermodynamics. As an original contribution, the potential energy of the saturated materials weakened by closed frictional microcracks is determined and formulated as a sum of an elastic part and a plastic part, the latter entirely induced by frictional sliding of microcracks. The influence of fluid pressure is accounted for in the friction criterion through the concept of local effective stress at microcracks. We show that the Biot's effective stress controls the evolution of total strain while the local Terzaghi's effective stress controls the evolution of plastic strain. Further, the frictional sliding between crack lips generates volumetric dilatancy and reduction in fluid pressure. Applications of the proposed model to typical brittle rocks are presented with comparisons between numerical results and experimental data in both drained and undrained triaxial tests.

1. Introduction

Damage induced by microcracks is an essential mechanism of inelastic deformation and failure in most cohesive geomaterials such as concrete and rocks. In many engineering applications, these materials are not only subjected to mechanical loads but also to variation of pore pressure. The mechanical behavior and poromechanical coupling properties as well as permeability are strongly affected by the induced damage. On the other hand, the damage evolution is controlled by mechanical loads and pore pressure variation. Therefore, it is essential to investigate such coupling phenomena for the analysis of failure and fluid flow in many engineering applications. The present paper intends to propose a micromechanical analysis of damage evolution and related inelastic deformation in quasi brittle materials in saturated conditions. In particular, we will focus at the case of closed cracks under compressive stresses, which is still open issue.

In the last decades, a number of phenomenological models have been proposed for quasi brittle geomaterials (we do not intend to give an exhaustive list here). These models are generally based on macroscopic experimental data and formulated in the framework of irreversible thermodynamics. The damage state is characterized by scalar or tensorial internal variables. In some cases, the physical significance of such internal variables is not always clearly defined. With a relatively high number of parameters, the phenomenological damage models can provide an efficient tool for modeling main features of mechanical behaviors of geomaterials. They are now used in failure analysis of various engineering structures. Further, some extensions have also been proposed for damage modeling in saturated and partially saturated porous geomaterials (Shao, 1998; Bourgeois et al., 2002; Shao et al., 2004; Kuhl et al., 2004; Selvadurai, 2004; Xie and Shao, 2006; Maleki and Pouya, 2010 to mention a few). However, with the phenomenological approaches, the physical phenomena at different scales, which represent the origin of material damage and inelastic deformation, are not properly taken into account. Due to this, there are some difficulties in phenomenological models to properly consider some important features of material behavior, for example, inherent damage-friction coupling, unilateral effects and related continuity at the opening-closing transition of cracks, volumetric dilatation induced by frictional sliding, hysteretic loop related to local hardening kinetics. Therefore, micromechanics-based constitutive models have been developed and applied to induced damage in cohesive geomaterials (Mura, 1987; Kachanov, 1992; Gambarotta and Lagomarsino, 1993; Nemat-Nasser and Hori,

* Corresponding author.
E-mail address: jianfu.shao@univ-lille1.fr (J.F. Shao).

0020-7683/$ - see front matter © 2012 Elsevier Ltd. All rights reserved.
doi:10.1016/j.ijsolstr.2011.12.006

1993; Lubarda and Krajcinovic, 1993; Ju and Chen, 1994; Basista and Gross, 1998; Brancich and Gambarotta, 2001; Pensee et al., 2002; Golshani et al., 2006; Marmier et al., 2007; Abou-Charka Guery et al., 2008; Zhu et al., 2008a,b, just to mention a few). These models were attempted to improve phenomenological modeling by incorporating different modes of distribution and propagation of microcracks. The micromechanical models provide an alternative way for damage modeling in brittle materials. However, most models developed so far have been essentially applied to dry materials. Few studies are conducted on micromechanical modeling of damage in saturated or partially geomaterials. Dormieux and his coworkers were among founding researchers to have developed micromechanics of damage in saturated brittle media (Dormieux et al., 2006; Dormieux and Kondo, 2007). However, their works are still limited to the cases of opened cracks or closed frictionless cracks in elastic solid matrix. In these two conditions, the deformation of both cracks and matrix are elastic, implying that the free energy of the RVE is reversible. More recently, interesting progresses have been achieved by Zhu et al. (2011) in micromechanics-based modeling of coupled friction-induced inelastic deformation and damage in quasi-brittle materials under dry condition. However, the interaction between elastoplastic deformation and interstitial fluid pressure variation has not yet been dealt with in their works.

The present work is devoted to extending the previous work of Zhu et al. (2011) to micromechanical modeling of poromechanical behavior in saturated quasi-brittle rocks with the emphasis on the coupling between friction-induced plasticity, damage evolution as well as variation of interstitial fluid pressure. We will essentially focus on closed microcracks under compressive stresses. Damage is directly related to the frictional sliding along rough crack surfaces. We first derive the macroscopic potential energy for the RVE of cracked solids for the case of opened cracks. The obtained result is then extended to the case of closed saturated microcracks. Applying the thermodynamics to local scale, frictional sliding criterion and damage evolution law will be formulated. The Ponte–Castaneda and Willis homogenization scheme (Ponte-Castaneda and Willis, 1995) will be used for the determination of effective properties of damaged materials. After the identification of model's parameters, the proposed model will be applied to simulate coupled poromechanical tests performed on typical porous quasi-brittle rocks in both drained and undrained conditions.

2. Description of micro-cracked media

Let us consider a cracked porous cohesive material. The representative elementary volume (REV), denoted by Ω, is composed of a solid matrix and a random distribution of defects. According to their shapes, these defects in the matrix can be mainly classified into two categories, i.e. flat openings, assumed to be penny-shaped, which we call cracks, and rounded openings, which we call pores. In this work, the ensemble of the solid phase and pores therein is taken as a homogenized porous matrix, for the reason that focus here is put on the characterization of inelastic behaviors induced by microcracking (characterized by damage variable) and its coupling with friction-induced plasticity. Thus, the REV on which the current study relies is composed of a pores-weakened solid matrix and distributed microcracks, as shown in Fig. 1a.

The pores-weakened matrix is assumed to be linearly elastic with the elasticity tensor $\mathbb{C}^m$, which is, more or less, softer than the elasticity tensor $\mathbb{C}^s$ of the solid phase. Inelastic behavior, material degradation and failure process are viewed as the consequence of propagation of microcracks. Approximated by oblate inclusions, microcracks are, according to their normal directions, classified into M families with elasticity tensor $\mathbb{C}^{c,r}$ for the rth crack family. When cracks are closed, the evolution of inelastic deformations will occur only when some condition of frictional sliding is met, while for open cracks nonlinear properties in the elementary volume are caused by elastic damage. Moreover, crack's opening/closure state depends on local unilateral contact condition.

For micromechanical determination of material effective properties, it is possible to make direct use of the basic solution to the Eshelby's inclusion problem. By adopting local linearly elastic constitutive behavior for both the matrix and inclusions (cracks), the effective elasticity tensor $\mathbb{C}^{\hom}$ of the cracks-matrix system is classically obtained by taking average of the local stiffness over the whole domain Ω (Zaoui, 2002; Dormieux et al., 2006; Zhu et al., 2009):

$$\mathbb{C}^{\hom} = \mathbb{C}^m + \sum_{r=1}^{M} \varphi^{c,r}(\mathbb{C}^{c,r} - \mathbb{C}^m) : \mathbb{A}^{c,r}, \tag{1}$$

where $\varphi^{c,r}$ and $\mathbb{A}^{c,r}$ are the volume fraction and the averaged concentration tensor of the rth crack family, respectively. $\mathbb{A}^{c,r}$ relates the local strain ε linearly to the macroscopic one $\boldsymbol{E}$, i.e. $\varepsilon = \mathbb{A}^c : \boldsymbol{E}$. Several homogenization schemes for deriving the concentration tensor can be found in the literature, for instance, the dilute scheme, the Mori–Tanaka scheme, the Ponte–Castaneda and Willis estimation and the self-consistent method.

Focus now on a family of penny-shaped microcracks of normal $\underline{n}^r$ and with the aspect ratio $\theta = c_r/a_r$, with a_r and c_r being, respectively, the radius and half height of the cracks, as illustrated in Fig. 1. When all microcracks are approximated as flat ellipsoids, the volume fraction $\varphi^{c,r}$ of the rth crack family reads

$$\varphi^{c,r} = \frac{4}{3}\pi a_r^2 c_r \mathscr{N}_r = \frac{4}{3}\pi\theta d_r, \tag{2}$$

where $\mathscr{N}_r$ denotes crack density (crack number per unit volume) and $d_r = \mathscr{N}_r a_r^3$ is the crack damage parameter (Budiansky and O'Connel, 1976). When limited to isotropic case, a scalar variable d, common to all crack families ($d_r = d$), will suffice to describe the process of material degradation. In this case, material damage is orientation-independent, corresponding to the case where a large number of microcracks are randomly distributed in the REV. For simplicity, the damage evolution is only related to the propagation of cracks by neglecting the change of pores.

3. Poroelasticity of saturated media with open cracks

In this work, the Ponte–Castaneda and Willis' homogenization scheme (PC-W) is adopted for its explicit form and the ability of properly taking into account the influence of spatial distribution of microcracks. When all microcracks in the REV are open, the global deformation is elastic and the effective elasticity tensor $\mathbb{C}^{\hom}$ is obtained by setting $\mathbb{C}^{c,r} = 0$ in Eq. (1) due to the cancellation of local stress within cracks. In the isotropic case, $\mathbb{C}^{\hom}$ can be expressed as the linear combination of the four order projection operators $\mathbb{J}$ and $\mathbb{K}$:

$$\mathbb{C}^{\hom} = 3k^{\hom}\mathbb{J} + 2\mu^{\hom}\mathbb{K}, \tag{3}$$

with

$$J_{ijkl} = \frac{1}{3} I_{ij} I_{kl}, \quad K_{ijkl} = I_{ijkl} - J_{ijkl},$$

where I_{ij} and I_{ijkl} are the components of the second and fourth order identity tensors, respectively. In Eq. (3), the effective module of compressibility $k^{\hom}$ and the effective shear module $\mu^{\hom}$ take the following form:

$$\mu^{\hom} = \mu^m\left(1 - \frac{\eta_2 d}{1 + \eta_2\alpha_2 d}\right); \quad k^{\hom} = k^m\left(1 - \frac{\eta_1 d}{1 + \eta_1\alpha_1 d}\right), \tag{4}$$

where μ^m and k^m are the shear and bulk modulus of the matrix, respectively; both η_1 and η_2 are functions of the Poisson's ratio of

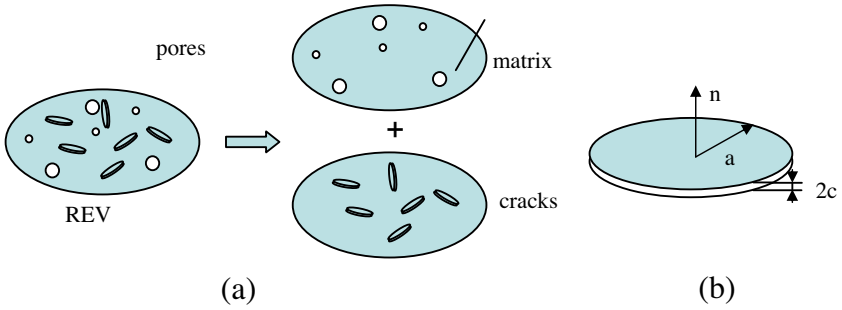

Fig. 1. (a) decomposition of the REV and (b) schematic representation of a penny-shaped crack.

solid matrix such that $\eta_1 = \frac{16(1-(\nu^m)^2)}{9(1-2\nu^m)}$ and $\eta_2 = \frac{32(1-\nu^m)(5-\nu^m)}{45(2-\nu^m)}$. The coefficients α_1 and α_2 are used to characterize the effect of spatial distribution of microcracks via the fourth tensor $\left(\frac{\alpha_1}{3k^m}\mathbb{J} + \frac{\alpha_2}{2\mu^m}\mathbb{K}\right)$, whose expressions in the isotropic case are given by $\alpha_1 = \frac{1}{3}\frac{1+\nu^m}{1-\nu^m}$ and $\alpha_2 = \frac{2}{15}\frac{4-5\nu^m}{1-\nu^m}$. Note that unlike the scalar damage variable d widely used in the macroscopic phenomenological damage theory, which generally varies from 0 to the critical value 1, the damage variable in the present micromechanical analysis is physically related to the microcrack density as mentioned in the relation (2). In the isotropic case, the damage variable is defined as $d = Na^3/|\Omega|$ where a denotes the mean radius of penny-shaped microcracks and $N/|\Omega|$ is the crack density (crack number per unit volume) in the representative volume under consideration. Therefore, although the volume fraction for microcracks is generally very small because of their opening degree negligible with respect to the radius, the variable $Na^3/|\Omega|$ may be not limited to the unity. In fact, the critical value, corresponding to which the elastic modulus decreases to zero, is dependent on the choice of homogenization scheme.

When the cracked porous material is saturated by interstitial fluid, the REV is subjected to both the macroscopic uniform strain $\boldsymbol{E}$ on its boundary $\partial\Omega$ and to the fluid pressure$p$ at the solid–fluid interface. Accordingly the work rate is expressed as:

$$\dot{\Psi}_s = \boldsymbol{\Sigma} : \dot{\boldsymbol{E}} + p\dot{\phi} \tag{5}$$

where ϕ is the porosity of the REV. $\boldsymbol{\Sigma} : \dot{\boldsymbol{E}}$ denotes the strain work rate in absence of water pressure and $p\dot{\phi}$ the work rate generated by interstitial pressure. The stress tensor is function of the macroscopic strain and the pressure

Under isothermal conditions and the assumption of small strains, the macroscopic elastic free energy density Ψ_s takes the following form Coussy (2004), Dormieux and Kondo (2007):

$$\Psi_s = \boldsymbol{\Sigma} : \boldsymbol{E} + p(\phi - \phi_0) = \frac{1}{2}\boldsymbol{E} : \mathbb{C}^{\text{hom}} : \boldsymbol{E} + \frac{p^2}{2N}s \tag{6}$$

where use has been made of the relations

$$\boldsymbol{\Sigma} = \boldsymbol{E} : \mathbb{C}^{\text{hom}} - p\boldsymbol{B}, \quad \dot{\phi} = \boldsymbol{B} : \dot{\boldsymbol{E}} + \frac{\dot{p}}{N} \tag{7}$$

The corresponding potential energy Ψ_s^* is derived by a simple transformation:

$$\Psi_s^* = \Psi_s - p(\phi - \phi_0) = \frac{1}{2}\boldsymbol{E} : \mathbb{C}^{\text{hom}} : \boldsymbol{E} - \frac{p^2}{2N} - p\boldsymbol{B} : \boldsymbol{E} \tag{8}$$

Note that $\frac{1}{N}$ and $\boldsymbol{B}$ are the well-known Biot modulus and the tensor of Biot coefficients, respectively (Biot and Willis, 1957; Nur and Byerlee, 1971). Under drained conditions, both $\frac{1}{N}$ and $\boldsymbol{B}$ are functions of the homogenized elasticity tensor $\mathbb{C}^{\text{hom}}$ (Dormieux and Kondo, 2007):

$$\boldsymbol{B} = \boldsymbol{I} - \mathbb{C}^{\text{hom}} : \mathbb{S}^s : \boldsymbol{I} \tag{9}$$

$$\frac{1}{N} = (\boldsymbol{B} - \phi\boldsymbol{I}) : \mathbb{S}^s : \boldsymbol{I} \tag{10}$$

where $\mathbb{S}^s = (\mathbb{C}^s)^{-1}$ is the elastic compliance tensor of the solid phase of the REV, and ϕ_0 is the initial porosity. By making use of (3) and (4), Eqs. (8) and (9) are further rewritten as:

$$B = \left(1 - \frac{k^{\text{hom}}}{k^s}\right)\boldsymbol{I} = \left(1 - \frac{k^m}{k^s}\right)\boldsymbol{I} + \frac{k^m}{k^s}\frac{\eta_1 d}{1 + \eta_1\alpha_1 d}\boldsymbol{I}, \tag{11}$$

$$\frac{1}{N} = \frac{1}{k^s}\left(1 - \frac{k^{\text{hom}}}{k^s} - \phi\right). \tag{12}$$

Thus, the Biot coefficient $\boldsymbol{B}$ can be divided into two parts

$$\boldsymbol{B} = \boldsymbol{B}_0 + \boldsymbol{B}(d) = b_0\boldsymbol{I} + (1 - b_0)\frac{\eta_1 d}{1 + \eta_1\alpha_1 d}\boldsymbol{I}, \tag{13}$$

with $b_0 = 1 - \frac{k^m}{k^s}$. The first part $\boldsymbol{B}_0$ represents the Biot coefficients due to the existence of pores (Biot and Willis, 1957), and the second part $\boldsymbol{B}(d)$ corresponds to the contribution by microcracks.

In the framework of thermodynamics, the macroscopic stress–strain relationship and the relative variation of porosity are derived by standard differentiation of the potential energy

$$\boldsymbol{\Sigma} = \frac{\partial\Psi_s^*}{\partial\boldsymbol{E}} = \mathbb{C}^{\text{hom}} : \boldsymbol{E} - \boldsymbol{B}p, \tag{14}$$

$$\phi - \phi_0 = -\frac{\partial\Psi_s^*}{\partial p} = \frac{p}{N} + \boldsymbol{B} : \boldsymbol{E}. \tag{15}$$

The above poroelastic relations hold for the case of saturated media with open cracks. However, in most cases, porous quasi brittle materials like concrete and rocks are generally subjected to compression-dominated stresses leading to closure of microcracks. Due to local tangential stresses, frictional sliding may occur along rough crack faces, usually accompanied by crack propagation leading to damage evolution of material. Further, normal opening can be generated by tangential sliding due to asperities of crack surfaces and such an opening leads to macroscopic volumetric dilation. Therefore, the above results should be extended to the case of closed cracks saturated by interstitial fluid, by taking into account the coupling between damage evolution and dissipative frictional sliding.

4. Micromechanical formulation for closed microcracks

This section is devoted to the description of inelastic behavior of saturated media with frictional microcracks in open and closed states. In the case of closed cracks, the most previous works generally considered idealized smooth cracks without friction (Dormieux et al., 2006; Zhu et al., 2008a,b). However, as mentioned above, in real cases, both inherent and induced cracks in geomaterials contain

rough surfaces with various forms of asperities. The local friction coefficient depends on the evolution of such asperities. On the other hand, the frictional sliding along rough cracks can generate both normal aperture and tangential sliding. Unlike the poroelastic behavior of open cracks, the strains related to displacement discontinuities on cracks are no long available. We thus propose to determine the evolution of such strains within the framework of plasticity theory. Based on previous works (Zhu et al., 2008a,b), we propose to combine the homogenization procedure for the determination of effective properties and the standard thermodynamics framework for the dissipation process related to frictional sliding. For this purpose, it appears convenient to determine first the macroscopic free energy with consideration of the influence of interstitial pressure. Since the present problem is a dissipative one, we chose to formulate the constitutive equations in a rate-dependent form (Lubarda and Krajcinovic, 1995; Dormieux and Kondo, 2007).

For the clarity of presentation, we start with one family of microcracks with unit normal vector $\underline{n}$. As mentioned above, the frictional sliding along cracks is described as a plastic phenomenon and a normal opening can be generated due to the roughness of crack surfaces. Denote the averaged opening and the vector of relative sliding between two crack surfaces by β and $\underline{\gamma}$, respectively. Both β and $\underline{\gamma}$ are related to the displacement discontinuity $[\underline{u}]$ such that:

$$\beta = \mathscr{N}\int_{\partial\Omega_c}[\underline{u}].\underline{n}\,\mathrm{d}S;\ \underline{\gamma} = \mathscr{N}\int_{\partial\Omega_c}[\underline{u}].(\boldsymbol{I}-\underline{n}\otimes\underline{n})\,\mathrm{d}S. \tag{16}$$

The local inelastic strain ε^c then takes the form:

$$\varepsilon^c = \beta\underline{n}\otimes\underline{n} + \frac{1}{2}(\underline{\gamma}\otimes\underline{n} + \underline{n}\otimes\underline{\gamma}). \tag{17}$$

Furthermore, the macroscopic strain $\boldsymbol{E}^{pl}$ can be obtained by integration of $\varepsilon^c(\underline{n})$ over the surface of a unit sphere

$$\boldsymbol{E}^{pl} = \frac{1}{8\pi}\int_S [2\beta n\otimes n + (\underline{\gamma}\otimes\underline{n} + \underline{n}\otimes\underline{\gamma})]\,\mathrm{d}S. \tag{18}$$

Under the isotropic assumption, $\boldsymbol{E}^{pl}$ is finally decomposed into a spherical part and a deviatoric part (Zhu et al., 2011):

$$\boldsymbol{E}^{pl} = \frac{1}{3}\beta\boldsymbol{I} + \boldsymbol{\Gamma}, \tag{19}$$

with the relations

$$\beta = \mathrm{tr}\boldsymbol{E}^{pl},\quad \boldsymbol{\Gamma} = \frac{1}{8\pi}\int_{\partial\Omega^c}(\underline{\gamma}\otimes\underline{n} + \underline{n}\otimes\underline{\gamma})\,\mathrm{d}S. \tag{20}$$

Remark that the above formulations are valid for both open and closed cracks. The difference between these two cases states that for open cracks analytical solution for β and $\underline{\gamma}$ is available while for closed cracks it is not.

4.1. Problem decomposition

We now proceed to establish the macroscopic free energy in terms of the plastic strains $\boldsymbol{E}^{pl}$ and the interstitial pressure p. It is convenient to divide the macroscopic strain into two parts: the elastic strain of the matrix $(\boldsymbol{E}-\boldsymbol{E}^{pl})$ and the inelastic strain induced by the discontinuities of cracks $\boldsymbol{E}^{pl}$. Accordingly the initial problem is decomposed into two sub-problems, as illustrated in the Fig. 2.

In Sub-problem 1, the REV contains an elastic homogeneous matrix weakened by pores. In this matrix, both the stress and strain fields in the REV are uniform and expressed as:

$$\frac{1}{|\Omega|}\int_{\Omega^s}\dot{\varepsilon}^{(1)}\,\mathrm{d}V = \dot{\boldsymbol{E}} - \dot{\boldsymbol{E}}^{pl}. \tag{21}$$

$$\boldsymbol{\sigma}^{(1)} = \frac{1}{|\Omega|}\int_{\Omega^s}\mathbb{C}^m : \varepsilon^{(1)}\,\mathrm{d}V - p\boldsymbol{B}^{(1)} = \mathbb{C}^m : (\boldsymbol{E}-\boldsymbol{E}^{pl}) - p\boldsymbol{B}^{(1)} \tag{22}$$

The variation of porosity is totally elastic and can be calculated by using (15). Since in Sub-problem 1 the REV is only pores-weakened, the tensor of Biot coefficient takes the part B_0 of the Eq. (12), i.e.

$$\boldsymbol{B}^{(1)} = \boldsymbol{B}_0 = b_0\boldsymbol{I} \tag{23}$$

and correspondingly

$$\frac{1}{N^{(1)}} = \frac{1}{k^s}(b_0 - \phi_0) \tag{24}$$

Thus, the variation of porosity is the difference between $\phi^{(1)}$ and $\phi_0^{(1)}$

$$\phi^{(1)} - \phi_0^{(1)} = \phi^e = p\frac{b_0-\phi_0}{k^s} + b_0\mathrm{tr}(\boldsymbol{E}-\boldsymbol{E}^{pl}). \tag{25}$$

The rate form of the free energy in the matrix is finally obtained by (21), (22) and (25):

$$\dot{\Psi}_s^{(1)} = \frac{1}{\Omega}\int_{\Omega^s}\boldsymbol{\sigma}^{(1)} : \dot{\varepsilon}^{(1)}\,\mathrm{d}V + p\dot{\phi}^{(1)} = (\boldsymbol{E}-\boldsymbol{E}^{pl}) : \mathbb{C}^s : (\dot{\boldsymbol{E}} - \dot{\boldsymbol{E}}^{pl}) + p\dot{p}\frac{b_0-\phi_0}{k^s} \tag{26}$$

In the sub-problem 2, the local stress field $\boldsymbol{\sigma}^{(2)}$ is self-equilibrated and fluid-free, i.e.

$$\langle\boldsymbol{\sigma}^{(2)}\rangle_\Omega = 0, \tag{27}$$

The strain field $\varepsilon^{(2)}$ is assumed to be completely attributed to discontinuities by cracks, leading to the following relationship by using the homogenization procedure:

$$\frac{1}{\Omega}\int_{\Omega_c}\dot{\varepsilon}^{(2)}\,\mathrm{d}V = \dot{\boldsymbol{E}}^{pl} \tag{28}$$

According to Zhu et al. (2008a), the following relation between the local stress and the inelastic strain can be established:

$$\boldsymbol{\sigma}^{(2)} - p\boldsymbol{I} = -\mathbb{C}^{pl} : \boldsymbol{E}^{pl}, \tag{29}$$

with $\mathbb{C}^{pl} = [(\mathbb{I}-\mathbb{A}^c)^{-1} : \mathbb{A}^c : \mathbb{S}^m]^{-1}$. In isotropic case, the global strain concentration tensor $\mathbb{A}^c$ is given as:

$$\mathbb{A}^c = \frac{48(1-\nu^2)d}{27(1-2\nu)+16(1+\nu)^2d}\mathbb{J} + \frac{480(1-\nu)(5-\nu)d}{675(2-\nu)+64(5-\nu)(4-5\nu)d}\mathbb{K}. \tag{30}$$

And $\mathbb{C}^{pl}$ takes the general form:

$$\mathbb{C}^{pl} = 3k^b\mathbb{J} + 2\mu^b\mathbb{K}, \tag{31}$$

with the coefficients (Zhu et al., 2011):

$$k^b = \frac{1+\eta_1(\alpha_1-1)d}{\eta_1 d}k^m,\quad \mu^b = \frac{1+\eta_2(\alpha_2-1)d}{\eta_2 d}\mu^m.$$

According to the decomposition of free energy given in (43), the fourth order tensor $\mathbb{C}^{pl}$ characterizes the capability of storing the energy due to frictional sliding, and depends on the mechanical property of solid matrix and the current state of damage (density and size of cracks). All inelastic variation of porosity occurs in Sub-problem 2, leading to the relation:

$$\phi^{(2)} - \phi_0^{(2)} = \phi^{pl} = \frac{1}{|\Omega|}\int_{\Omega^c}\mathrm{tr}\varepsilon^{(2)}\,\mathrm{d}V. \tag{32}$$

It follows by comparing the above measure with (20):

$$\phi^{pl} = tr\boldsymbol{E}^{pl} = \beta. \tag{33}$$

By the definition of $\dot{\Psi}_s$, the rate of the free energy in the sub-problem 2 is expressed as follows:

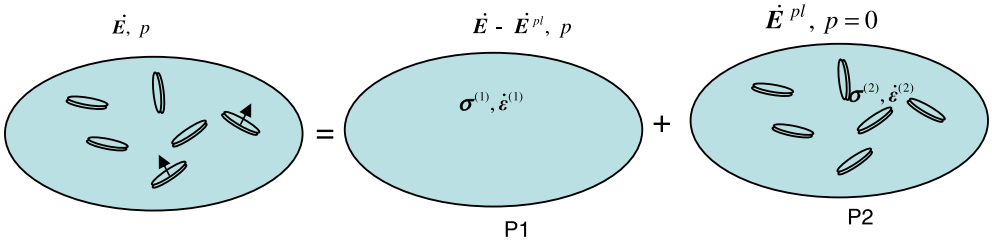

Fig. 2. Problem decomposition of a saturated porous media with microcracks.

$$\dot{\Psi}_s^{(2)} = \frac{1}{|\Omega|}\int_{\Omega^s} \boldsymbol{\sigma}^{(2)} : \dot{\varepsilon}^{(2)} dV + p\dot{\phi}^{(2)}. \tag{34}$$

Noting the relationship between the two sub-domains $\Omega^c \cup \Omega^s = \Omega$, the above equation is equivalent to the following form:

$$\dot{\Psi}_s^{(2)} = \frac{1}{|\Omega|}\int_{\Omega} \boldsymbol{\sigma}^{(2)} : \dot{\varepsilon}^{(2)}\, \mathrm{d}V - \frac{1}{|\Omega|}\int_{\Omega^c} \boldsymbol{\sigma}^{(2)} : \dot{\varepsilon}^{(2)}\, \mathrm{d}V + p\dot{\phi}^{(2)}. \tag{35}$$

By using (29) and (34) as well as the self-equilibrating property (27), the above equation gives

$$\dot{\Psi}_s^{(2)} = \boldsymbol{E}^{pl} : \mathbb{C}^{pl} : \dot{\boldsymbol{E}}^{pl}. \tag{36}$$

Note that $\dot{\Psi}_s^{(2)}$ is a function of plastic strain $\boldsymbol{E}^{pl}$ induced by microcracks, and is generally termed as the blocked free energy stocked in closed cracks.

4.2. Determination of the overall free energy

By combining $\dot{\Psi}_s^{(1)}$ and $\dot{\Psi}_s^{(2)}$, the overall free energy in the REV is finally obtained as

$$\begin{aligned}\dot{\Psi}_s &= \frac{1}{|\Omega|}\int_{\Omega^s} (\varepsilon^{(1)} + \varepsilon^{(2)}) : \mathbb{C}^m : (\dot{\varepsilon}^{(1)} + \dot{\varepsilon}^{(2)})\, \mathrm{d}V + p(\dot{\phi}^{(1)} + \dot{\phi}^{(2)}) \\ &= \dot{\Psi}_s^{(1)} + \dot{\Psi}_s^{(2)} + \frac{1}{|\Omega|}\int_{\Omega^s} \varepsilon^{(1)} : \mathbb{C}^m : \dot{\varepsilon}^{(2)}\, \mathrm{d}V + \frac{1}{|\Omega|}\int_{\Omega^s} \varepsilon^{(2)} : \mathbb{C}^m \\ &\quad : \dot{\varepsilon}^{(1)}\, \mathrm{d}V \end{aligned} \tag{37}$$

Note that both $\mathbb{C}^m : \dot{\varepsilon}^{(2)} = \dot{\boldsymbol{\sigma}}^{(2)}$ and $\mathbb{C}^m : \varepsilon^{(2)} = \boldsymbol{\sigma}^{(2)}$ are self-equilibrated and that $\varepsilon^{(1)}$ and its rate form $\dot{\varepsilon}^{(1)}$ are uniform. One then has:

$$\frac{1}{|\Omega|}\int_{\Omega^s} \varepsilon^{(1)} : \mathbb{C}^m : \dot{\varepsilon}^{(2)}\, \mathrm{d}V + \frac{1}{|\Omega|}\int_{\Omega^s} \varepsilon^{(2)} : \mathbb{C}^m : \dot{\varepsilon}^{(1)}\, \mathrm{d}V = 0. \tag{38}$$

The general formulation (37) reduces finally to the sum of the energy rates $\dot{\Psi}_s^{(1)}$and $\dot{\Psi}_s^{(2)}$, i.e.

$$\dot{\Psi}_s = \dot{\Psi}_s^{(1)} + \dot{\Psi}_s^{(2)}, \tag{39}$$

which verifies the requirement on problem decomposition.

The total free energy Ψ_s in the REV is obtained by integration and expressed as:

$$\Psi_s = \frac{1}{2}(\boldsymbol{E} - \boldsymbol{E}^{pl}) : \mathbb{C}^s : (\boldsymbol{E} - \boldsymbol{E}^{pl}) + \frac{1}{2}\mathbb{C}^{pl} : \boldsymbol{E}^{pl} : \boldsymbol{E}^{pl} + \frac{b_0 - \phi_0}{2k^s}p^2. \tag{40}$$

Recall the definition

$$\Psi_s^* = \Psi_s - p(\phi - \phi_0). \tag{41}$$

It follows by introducing (25), (33) and (40) into (41)

$$\begin{aligned}\Psi_s^* &= \frac{1}{2}(\boldsymbol{E} - \boldsymbol{E}^{pl}) : \mathbb{C}^s : (\boldsymbol{E} - \boldsymbol{E}^{pl}) + \frac{1}{2}\mathbb{C}^{pl} : \boldsymbol{E}^{pl} \\ &\quad : \boldsymbol{E}^{pl} - \frac{b_0 - \phi_0}{2k^s}p^2 - pb_0\mathbf{I} : (\boldsymbol{E} - \boldsymbol{E}^{pl}) - p\,\mathrm{tr}\boldsymbol{E}^{pl}. \end{aligned} \tag{42}$$

By setting $p = 0$, this potential energy reduces to that of dry materials (Zhu et al., 2008a, 2011):

$$\Psi_s^* = \frac{1}{2}(\boldsymbol{E} - \boldsymbol{E}^{pl}) : \mathbb{C}^s : (\boldsymbol{E} - \boldsymbol{E}^{pl}) + \frac{1}{2}\boldsymbol{E}^{pl} : \mathbb{C}^{pl} : \boldsymbol{E}^{pl} \tag{43}$$

The potential energy (42) contains a recoverable part stored in the solid matrix and a second part in form of the stored energy U due to closed microcracks

$$U = \frac{1}{2}\boldsymbol{E}^{pl} : \mathbb{C}^{pl} : \boldsymbol{E}^{pl} - p\,\mathrm{tr}\boldsymbol{E}^{pl} \tag{44}$$

Within the thermodynamic framework of irreversible processes, the state equations are then obtained by standard differentiation of potential energy with respect to the internal variables:

$$\boldsymbol{\Sigma} = \frac{\partial \Psi_s^*}{\partial \boldsymbol{E}} = \mathbb{C}^s : (\boldsymbol{E} - \boldsymbol{E}^{pl}) - b_0 p\mathbf{I}, \tag{45}$$

$$\phi - \phi_0 = -\frac{\partial \Psi_s^*}{\partial p} = \frac{b_0 - \phi_0}{k^s}p + b_0\,\mathrm{tr}(\boldsymbol{E} - \boldsymbol{E}^{pl}) + \mathrm{tr}\boldsymbol{E}^{pl}. \tag{46}$$

And the elastic variation of porosity can also be obtained as:

$$\phi - \phi^p - \phi_0 = -\frac{\partial(\Psi_s^* - U)}{\partial p} = p\frac{b_0 - \phi_0}{k^s} + b_0\,\mathrm{tr}(\boldsymbol{E} - \boldsymbol{E}^{pl}), \tag{47}$$

which is the same as that given in (25).

4.3. Discussions

Upon the above formulations, it is useful to address the following discussions and comparisons:

- From the macroscopic free energy (40), it is seen that when cracks are closed, the tensor of Biot coefficients is totally contributed by the pores inside the matrix and the closed cracks have no contribution to it. This result conforms to the simplifying assumption that in the matrix phase there is no additional inelastic deformation during frictional sliding. The influence of crack sliding upon the change of pores has been neglected in the present framework.
- According to the previous work by Coussy (2004), when irreversible deformation occurs in micro-cracked media, the strain $\boldsymbol{E}$ and the Lagrange porosity ϕ are no longer efficient to capture the current Skeleton energy Ψ_s. Internal variables, such as plastic strain $\boldsymbol{E}^{pl}$, plastic porosity ϕ^{pl} as well as damage variable d, must be involved in the formulation of skeleton energy Ψ to characterize the energy dissipation. Thus, the free energy of the matrix Ψ_s can be expressed in the following general form:

$$\Psi_s = W_s(\boldsymbol{E} - \boldsymbol{E}^{pl}, \phi - \phi^{pl}, d) + U \tag{48}$$

and the potential energy changes accordingly into the form:

$$\Psi_s^* = W_s(\boldsymbol{E} - \boldsymbol{E}^{pl}, \phi - \phi^{pl}, d) - p(\phi - \phi^{pl} - \phi_0) + U, \tag{49}$$

with the first part W_s representing the reversible energy supplied by external loads, and U the trapped energy, the latter will dissipate during plastic deformation. Formally, U should be a function of both

$\boldsymbol{E}^{pl}$ and ϕ^{pl} as well as damage variable d. Under isothermal conditions, U takes the general form as:

$$\mathrm{d}U = \mathrm{d}W^p = \sigma_{ij}\,\mathrm{d}\varepsilon^p_{ij} + p\,\mathrm{d}\phi^p. \tag{50}$$

Comparison between Eqs. (49) and (42) shows that the form of free energy obtained here by micromechanical analyses supports the macroscopic framework established by Coussy (2004).

4.4. Frictional sliding criterion

Inspired by previous works, the frictional sliding in geomaterials is generally governed by the generalized Coulomb type criterion. This criterion is adopted and applied here at the local scale to describe the frictional sliding along microcracks. Based on the extension of the formulation for dry cracked materials by Zhu et al. (2011) to the current saturated case, the thermodynamic force that controls the evolution of inelastic strain is obtained by:

$$\boldsymbol{F}^{pl} = -\frac{\partial \Psi^*_s}{\partial \boldsymbol{E}^{pl}} = \boldsymbol{\Sigma} - \mathbb{C}^{pl} : \boldsymbol{E}^{pl} + p\boldsymbol{I} \tag{51}$$

where use has been made of the definition (45) for making occurrence of the macroscopic stress tensor $\boldsymbol{\Sigma}$.

According to the results given in (45) and (51), it is shown that the thermodynamic forces conjugated with total strain and that with plastic strain are the Biot effective stress and local Terzaghi effective stress, respectively. Some more detailed discussions on the validity of effective stress concept in plastic theory and failure condition of saturated materials can be found in De Buhan and Dormieux (1996) and Lydzba and Shao (2002).

In order to express the Coulomb criterion, it is convenient to decompose the local stress tensor into a spherical part and a deviatoric part. By denoting $\sigma^{pl} = \frac{1}{3}\mathrm{tr}(\boldsymbol{F}^{pl})$ and $\boldsymbol{S}^{pl} = \mathbb{K} : \boldsymbol{F}^{pl}$, it is then possible to perform the following decomposition

$$\boldsymbol{F}^{pl} = \mathbb{J} : \boldsymbol{F}^{pl} + \mathbb{K} : \boldsymbol{F}^{pl} = \sigma^{pl}\boldsymbol{I} + \boldsymbol{S}^{pl}, \tag{52}$$

where $\sigma^{pl} = \Sigma_m - k^b\beta + p$ and $\boldsymbol{S}^{pl} = \boldsymbol{S} - 2\mu^b\boldsymbol{\Gamma}$ with $\Sigma_m = \mathrm{tr}\boldsymbol{\Sigma}/3$ and $\boldsymbol{S} = \boldsymbol{\Sigma} - \Sigma_m\boldsymbol{I}$ standing for the mean part and deviatoric part of the macroscopic stress, respectively.

The friction criterion is then expressed as a function of the thermodynamic force:

$$f = \|\boldsymbol{S}^{pl}\| + c_f\sigma^{pl} = \|\boldsymbol{S} - 2\mu^b\boldsymbol{\Gamma}\| + c_f(\Sigma_m - k^b\beta + p) \leqslant 0. \tag{53}$$

In this work, an associated plastic flow rule is adopted for frictional sliding. The elastic strain β and $\boldsymbol{\Gamma}$ can be easily determined by following the normality rule.

4.5. Damage criterion

The thermodynamic force associated with the overall damage variable d is derived from the free energy (40) or the potential energy (42):

$$F^d = -\frac{\partial \Psi^*_s}{\partial d} = -\frac{1}{2}\boldsymbol{E}^{pl} : \frac{\partial \mathbb{C}^{pl}}{\partial d} : \boldsymbol{E}^{pl}. \tag{54}$$

It can be seen from (54) that it is the cumulated plastic shearing along crack faces that drives the evolution of damage. The interstitial pressure p is not explicitly involved in the expression of F^d. However, it is known from (53) that the interstitial pressure p takes a part in the friction criterion. Thus, the damage evolution is also dependent on the interstitial pressure in an indirect way as the consequence of frictional sliding.

The damage criterion is chosen to be an exponential function of F^d as usually used for brittle materials such as concrete and rocks.

$$f_d = d_c - (d_c - d_0)[\exp(-c_1F^d)] - d \leqslant 0, \tag{55}$$

where d_0 and d_c are the initial threshold and critical value of damage variable respectively, and c_1 is a model parameter that controls the kinetics of damage evolution. The critical damage value can be determined from the following condition for the effective value of shear modulus $\mu^{\mathrm{hom}} \geqslant 0$ (Zhu et al., 2011):

$$d_c = \frac{1}{\eta_2(1-\alpha_2)} = \frac{675(2-\nu^m)}{32(5-\nu^m)(7-5\nu^m)} \tag{56}$$

5. Numerical simulations

In this section, we apply the proposed micromechanics-based model to simulate triaxial compression tests performed on samples of a typical porous brittle material, sandstone, under drained and undrained conditions.

There are totally 7 parameters in the present model: 5 parameters for mechanical behavior of dry materials and 2 for poromechanical coupling. The two elastic constants, i.e. Young's modulus E and Poisson's radio ν, are determined from the elastic part of the stress–strain curves in triaxial compression tests. The local friction coefficient c_f can be fitted by the envelope of peak stresses obtained from a series of triaxial compression tests under different confining pressures. The initial damage threshold d_0 describes the initial distribution of microcracks and can depend on the value of confining pressure. The parameter $c_1$is numerically fitted from the nonlinear part of stress–strain curves of triaxial compression tests. In the poromechanical formulation of saturated materials, two additional parameters are needed: the initial porosity ϕ_0 and the initial Biot coefficient b_0, both of which can be determined experimentally by various procedures (Hu et al., 2010).

Further, it is known that the elastic modulus of porous sandstone is generally influenced by the confining pressure. The higher the confining pressure is, the greater the elastic modulus will be. In the present micromechanics-based model, the initial damage value will be adjusted to account for the variation of elastic modulus with the different confining pressure. Therefore, the initial damage threshold is defined as a parameter reflecting the damage state after the exertion of hydrostatic confining pressure, leading to progressive closure of microcracks. During the process of deviatoric loading, the damage variable d will increase with the propagation of microcracks.

5.1. Drained tests

As the variation of interstitial pressure is not studied in drained tests, the two coupling parameters, ϕ_0 and b_0, are not needed. The parameters for the sandstone used in drained tests are determined following the general procedure mentioned above and the values obtained are: $E = 21000$ MPa, $\nu = 0.23$, $c_1 = 1.0$, $c_f = 0.7$. The values of initial damage value for different confining pressures are as follows: $d_0 = 0.22$, 0.15, 0.001 and 0.001 for $p_c = 10$ MPa, 20 MPa, 30 MPa, 40 MPa respectively. Note that the value of initial damage density represents here the state of open microcracks in the samples after the application of confining pressure. It decreases when the confining pressure increases due to progressive closure of initial microcracks. Under high confining pressure, for instance 30 and 40 MPa, the initial microcracks inside sandstone are nearly completely closed and the corresponding damage density vanishes. However, from a computational point of view, a non-vanished value of initial damage is needed. Therefore a small value of $d_0 = 0.001$ is chosen in the simulation of the tests under 30 and 40 MPa confining pressures. Note that for application of the model to engineering boundary values problems, the damage state after confining pressure is generally not known a priori. We need to use some in situ geophysical data. For instance, it is possible to

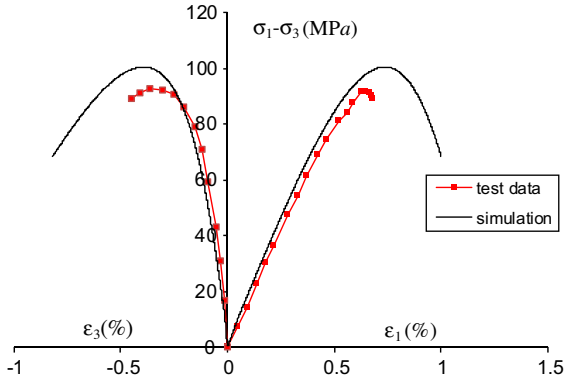

Fig. 3a. Stress–strain curves in drained triaxial compression test with 10 MPa confining pressure and comparison between numerical results (continuous lines) and experimental data.

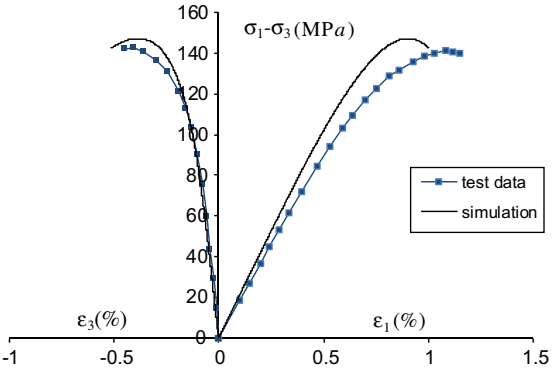

Fig. 3c. Stress–strain curves in drained triaxial compression test with 30 MPa confining pressure and comparison between numerical results (continuous lines) and experimental data.

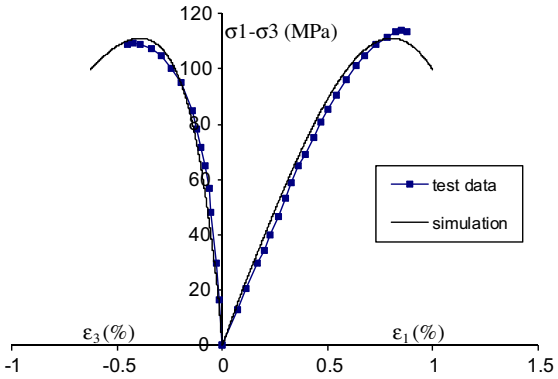

Fig. 3b. Stress–strain curves in drained triaxial compression test with 20 MPa confining pressure and comparison between numerical results (continuous lines) and experimental data.

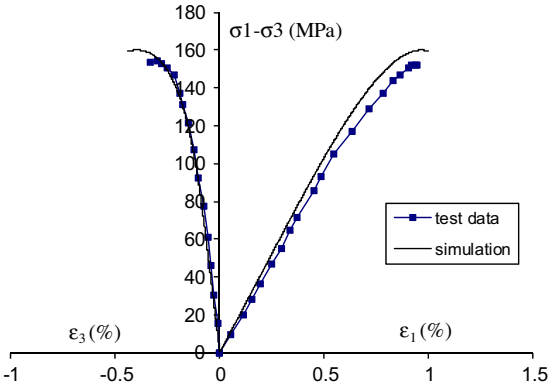

Fig. 3d. Stress–strain curves in drained triaxial compression test with 40 MPa confining pressure and comparison between numerical results (continuous lines) and experimental data.

choose an initial state of microcracks, and consider closing of microcracks. This method was used in some previous works concerning applications of micromechanical damage models to engineering problems (Pensee et al., 2002; Zhu et al., 2008b). An initial state of microcracks, generally uniform, was considered and all cracks were assumed to be closed under compression dominant stresses. However, the determination of initial state is another issue which is not addressed in detail here.

The mechanical response of the sandstone under drained condition is first simulated. The numerical results are compared with experimental data as shown in Figs. 3a–3d. It can be seen that both axial and lateral strains are in good agreement with the experimental data for different confining pressures. The proposed model seems to capture the main features of mechanical behavior of sandstone: inelastic deformation induced by crack propagation and sliding, pressure dependency, transition from volumetric compaction to dilatancy. In Fig. 4, we show the evolution of overall damage versus axial strain respectively in different triaxial compression tests with different confining pressures. We can see that the damage evolution is affected by confining pressure. The damage propagation threshold under deviatoric stress increases when the confining pressure is higher leading to smaller cumulated damage in material.

5.2. Undrained triaxial tests

By the extension of poroelastic theory to saturated brittle materials with inelastic deformation due to frictional sliding, the variation of interstitial pressure is given by:

$$\dot{p} = M\left(-btr(\dot{\mathbf{E}} - \dot{\mathbf{E}}^{pl}) + \frac{\dot{m}_f}{\rho_f} - \dot{\phi}^p\right), \tag{57}$$

in which m_f is the mass content variation of interstitial fluid with respect to a referential state, ρ_f is the density of the fluid, and M is the Biot modulus which is defined by $\frac{1}{M} = \frac{1}{N} + \frac{\phi}{k_f}$, with k_f standing for the bulk modulus of the fluid. According to the range of pressure and temperature considered here, the compressibility modulus of water in room temperature is used for interstitial fluid, i.e. $k_f = 2200$ MPa.

In an undrained triaxial compression test, there is no mass exchange of interstitial fluid and we have $\dot{m}_f$ in (57). The variation rate of interstitial pressure becomes:

$$\dot{p} = M(-btr\dot{\mathbf{E}} + b\dot{\beta} - \dot{\beta}) \tag{58}$$

where use has been made of the relation $\phi^p = \mathrm{tr}\mathbf{E}^{pl} = \beta$. One can see that the volumetric dilation generated by the frictional sliding between crack lips induces a reduction in interstitial pressure. The variation of interstitial pressure is inherently coupled with the mechanical response of the material. Once the elastic and plastic strains are derived, the variation of interstitial pressure can be obtained by the constitutive law. On the other hand, the variation of interstitial pressure has an effect on the frictional sliding condition and then influences the evolution of plastic strain. Further, it seems that the set of parameters for mechanical modeling of saturated sandstone is slightly different from that used for dry sandstone used in drained tests. For the sandstone used in undrained tests, the

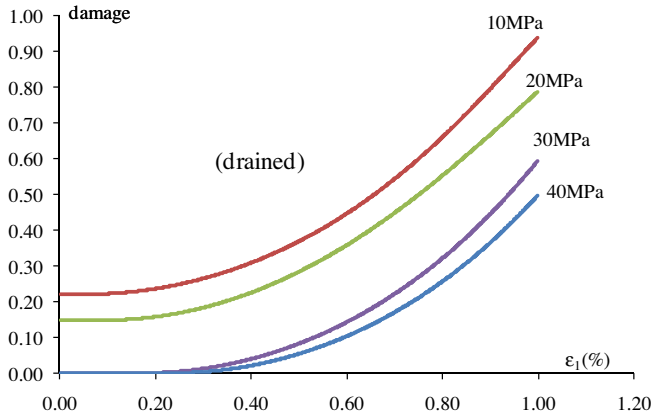

Fig. 4. Evolution of overall damage versus axial strain in drained tests with different confining pressures.

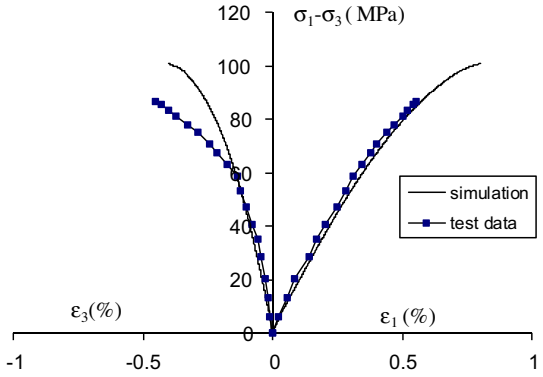

Fig. 5a. Stress–strain curves in undrained triaxial compression test with 10 MPa confining pressure and comparison between numerical results (continuous lines) and experimental data.

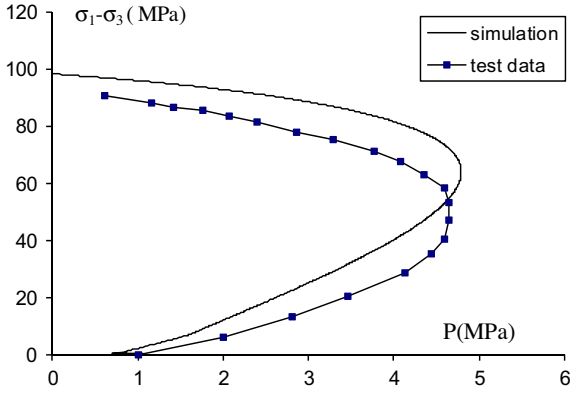

Fig. 5b. Interstitial pressure versus deviatoric stress in undrained triaxial compression test with 10 MPa confining pressure and comparison between numerical results (continuous lines) and experimental data.

following parameters are used: $E = 21000$ MPa, $\nu = 0.25$, $c_1 = 0.75$, $c_f = 0.5$, $\phi_0 = 0.12$, $b_0 = 0.8$.

Such a difference can be related to the fact that the samples used in the drained and undrained tests are not drilled exactly from the same block and there exists some heterogeneity between tested samples. Concerning the choice of the initial damage state for various confining pressures, we have adopted the same values as those used for drained tests presented in the preceding section. Thus the initial damage value is equal to $d_0 = 0.22$ for the confining pressure

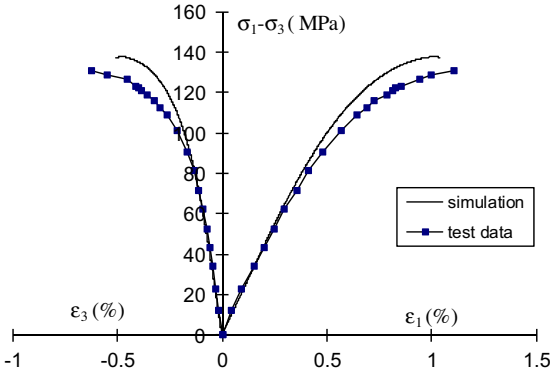

Fig. 6a. Stress–strain curves in undrained triaxial compression test with 30 MPa confining pressure and comparison between numerical results (continuous lines) and experimental data.

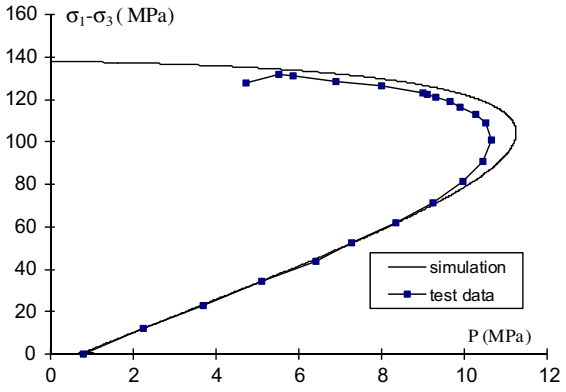

Fig. 6b. Interstitial pressure versus deviatoric stress in undrained triaxial compression test with 30 MPa confining pressure and comparison between numerical results (continuous lines) and experimental data.

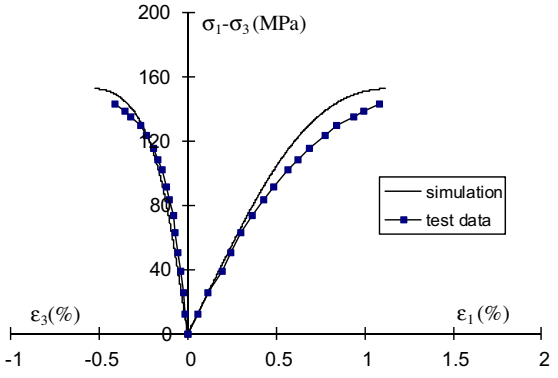

Fig. 7a. Stress–strain curves in undrained triaxial compression test with 50 MPa confining pressure and comparison between numerical results (continuous lines) and experimental data.

of 10 MPa. Under the confining pressures of 30 MPa and 50 MPa, experimental observations show that the initially existing cracks are nearly closed after the application of confining pressure. A small value of $d_0 = 0.001$ is used for the reason of computational convenience.

The numerical results are compared with experimental data for three values of confining pressures and respectively shown in Figs. 5a–7b. Again there is a good concordance both for strains and interstitial pressure. In particular, we can see that under deviatoric loading the interstitial pressure first increases and then

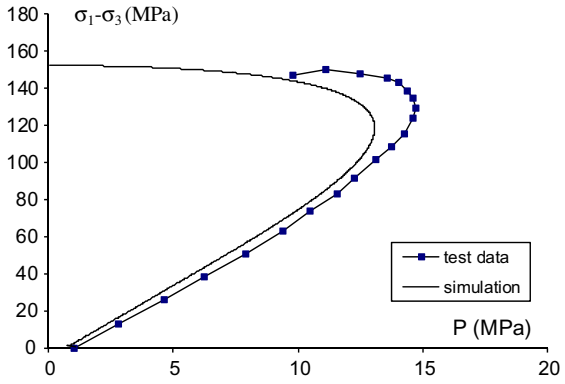

Fig. 7b. Interstitial pressure versus deviatoric stress in undrained triaxial compression test with 50 MPa confining pressure and comparison between numerical results (continuous lines) and experimental data.

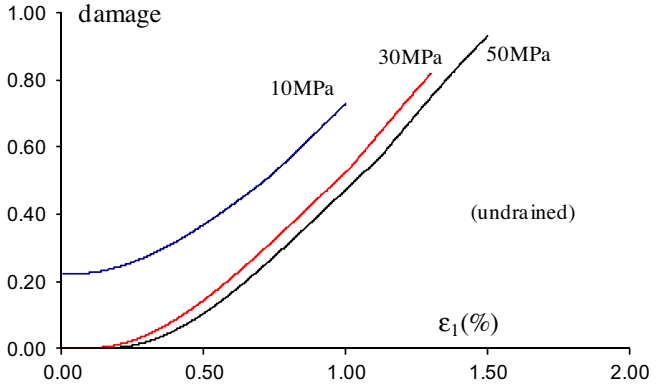

Fig. 8. Evolution of overall damage versus axial strain in undrained tests with different confining pressures.

decreases. This transition of interstitial pressure is in agreement with that of volumetric strain which evolves from compaction to dilation. The volumetric dilation is generated by the frictional sliding along crack faces and significantly intensified by the coalescence of microcracks in the zone near to the peak stress. The corresponding interstitial pressure tends in an asymptotical way toward to zero near the peak strength. In the present simulation, we choose to stop the calculation once the fluid pressure becomes zero in order to avoid various features related to strain localization. The evolution of damage versus axial strain is shown in Fig. 8 and similar remarks can be drawn as for drained tests.

6. Conclusions

A new micromechanical model is proposed for the description of damage evolution and plastic deformation in saturated porous quasi brittle materials. The macroscopic free energy of the REV is derived by combining the Eshelby's solution-based homogenization procedure with the thermodynamics of irreversible process. It is shown that the macroscopic energy is composed of an elastic part and a locked plastic part which is related to frictional sliding along closed microcracks. The damage evolution is therefore totally controlled by the frictional sliding, which is also the origin of volumetric dilatation. It is shown that the volumetric dilation due to frictional sliding affects the variation of interstitial pressure and in a coupled way the frictional sliding condition is influenced by the interstitial pressure.

Compared with most phenomenological models, the proposed micromechanical model contains a smaller number of parameters. The physical significance of each parameter is clearly defined. Further, the micromechanical model takes into account various physical mechanisms involved at relevant materials scales.

The proposed model has been used in the simulation of laboratory tests on sandstone in drained and undrained conditions. There was a good agreement between numerical results and experimental data. The proposed model is able to reproduce the main features of mechanical behavior and poromechanical coupling in saturated quasi-brittle materials. A number of future works can be envisaged: extension of the present work to anisotropic distribution of damage, coupling between microcracks and permeability evolution as well as extension to partially saturated media.

Acknowledgements

The authors are grateful for the financial supports by National Natural Science Foundation of China under the Grant Nos. 50778138 and 50911130366, and by the French ANR project MELANI. Ni XIE is grateful to China Scholarship Council for providing her a scholarship during her stay in France.

References

Abou-Charka Guery, A., Cormery, F., Shao, J.F., Kondo, D., 2008. A micromechanical model of elastoplastic and damage behaviour of a cohesive geomaterials. Int. J. Solids Struct. 45 (5), 1406–1429.
Basista, M., Gross, D., 1998. The sliding crack model of brittle deformation: an internal variable approach. Int. J. Solids Struct. 35 (5–6), 487–509.
Biot, M.A., Willis, D.G., 1957. The elastic coefficients of the theory of consolidation. ASME J. Appl. Mech. 24, 594–601.
Bourgeois, F., Burlion, N., Shao, J.F., 2002. Modelling of elastoplastic damage in concrete due to desiccation shrinkage. Int. J. Numer. Anal. Methods Geomech. 26, 759–774.
Brancich, A., Gambarotta, L., 2001. Isotropic damage model with different tensile-compressive response for brittle materials. Int. J. Solids Struct. 38, 5865–5892.
Budiansky, B., O'Connel, J., 1976. Elastic moduli of a cracked solid. Int. J. Solids Struct. 12, 81–97.
Coussy, O., 2004. Poromechanics. John Wiley & Sons Ltd.
De Buhan, P., Dormieux, L., 1996. On the validity of the effective stress concept for assessing the strength of saturated porous materials: a homogenization approach. J. Mech. Phys. Solids 44, 1649–1667.
Dormieux, L., Kondo, D., 2007. Micromechanics of damage propagation in fluid-saturated media. Revue européenne de Génie Civil 11, 945–962.
Dormieux, L., Kondo, D., Ulm, F.J., 2006. Microporomechanics. John Wiley & Sons.
Gambarotta, L., Lagomarsino, S., 1993. A microcrak damage model for brittle materials. Int. J. Solids Struct. 30 (2), 177–198.
Golshani, A., Okui, Y., Oda, M., 2006. A micromechanical model for brittle failure of rock and its relation to crack growth observed in triaxial compression tests of granite. Mech. Mater. 38, 287–303.
Hu, D.W., Zhou, H., Zhang, F., Shao, J.F., 2010. Evolution of poroelastic properties and permeability in damaged sandstone. International J. Rock Mech. Min. Sciences 47 (6), 962–973.
Ju, J.W., Chen, T.M., 1994. Effective elastic moduli of two-dimensional brittle solids with interacting microcracks, Part I: Basic formulations, Part II: Evolutionary damage models. J. Appl. Mech. 61, 349–366.
Kachanov, M., 1992. Effective elastic properties of cracked solid: critical review of some basic concepts. App. Mech. Rev. ASME 45 (8), 304–335.
Kuhl, D., Bangert, F., Meschke, G., 2004. Coupled chemo- mechanical deterioration of cementitious materials, Part I: Modeling. Int. J. Solids Struct. 41, 15–40.
Lubarda, V.A., Krajcinovic, D., 1993. Damage tensor and the crack density distribution. Int. J. Solids Struct. 30 (20), 2859–2877.
Lubarda, V.A., Krajcinovic, D., 1995. Constitutive structure of rate theory of damage in brittle elastic solids. Appl. Math. Comput. 67, 81–101.
Lydzba, D., Shao, J.F., 2002. Stress equivalence principle for saturated porous media. C.R. Mécanique 330, 297–303.
Maleki, K., Pouya, A., 2010. Numerical simulation of damage-permeability relationship in brittle geomaterials. Comput. Geotech. 37 (5), 619–628.
Marmier, R., Jeannin, L., Barthélémy, J.F., 2007. Homogenized constitutive laws for rocks with elastoplastic fractures. Int. J. Numer. Anal. Methods Geomech. 31, 1217–1237.
Mura, T., 1987. Micromechanics of Defects in Solids, 2nd ed. Martinus Nijhoff Pub., The Hague, Boston.
Nemat-Nasser, S., Hori, M., 1993. Micromechanics: Overall Properties of Heterogeneous Materials. North-Holland.
Nur, A., Byerlee, J.D., 1971. An exact effective stress law for elastic deformation of rock with fluids. J. Geophys. Res. 76, 6414–6419.
Pensee, V., Kondo, D., Dormieux, L., 2002. Micromechanical analysis of anisotropic damage in brittle materials. J. Eng. Mech. ASCE 128 (8), 889–897.

Ponte-Castaneda, P., Willis, J.R., 1995. The effect of spatial distribution of effective behavior of composite materials and cracked media. J. Mech. Phys. Solids 43, 1919–1951.

Selvadurai, A.P.S., 2004. Stationary damage modelling of poroelastic contact. Int. J. Solids Struct. 41, 2043–2064.

Shao, J.F., 1998. Poroelastic behaviour of brittle rock materials with anisotropic damage. Mech. Mater. 30, 41–53.

Shao, J.F., Lu, Y.F., Lydzba, D., 2004. Damage modeling of saturated rocks in drained and undrained conditions. J. Eng. Mech. ASCE 130 (6), 733–740.

Xie, S.Y., Shao, J.F., 2006. Elastoplastic deformation of a porous rock and water interaction. Int. J. Plast. 22, 2195–2225.

Zaoui, A., 2002. Structural morphology and constitutive behavior of microheterogeneous materials. In: Suquet, P. (Ed.), Continuum Micromechanics. Springer, New-York, pp. 91–347.

Zhu, Q.Z., Kondo, D., Shao, J.F., 2008a. Micromechanical analysis of coupling between anisotropic damage and friction in quasi brittle materials: role of the homogenization scheme. Int. J. Solids Struct. 45 (5), 1385–1405.

Zhu, Q.Z., Kondo, D., Shao, J.F., Pensée, V., 2008b. Micromechanical modelling of anisotropic damage in brittle rocks and application. Int. J. Rock Mech. Min. Sci. 45, 467–477.

Zhu, Q.Z., Kondo, D., Shao, J.F., 2009. Homogenization-based analysis of anisotropic damage in brittle materials with unilateral effect and interactions between microcracks. Int. J. Numer. Anal. Meth. Geomech. 33 (6), 749–772.

Zhu, Q.Z., Shao, J.F., Kondo, D., 2011. A micromechanics-based thermodynamic formulation of isotropic damage with unilateral and friction effects. Euro. J. Mech. A/Solids 30 (3), 316–325.